

## REVIEW

[View Article Online](#)  
[View Journal](#) | [View Issue](#)Cite this: *Mater. Adv.*, 2024,  
5, 7113Received 11th June 2024,  
Accepted 1st August 2024

DOI: 10.1039/d4ma00604f

[rsc.li/materials-advances](https://rsc.li/materials-advances)

# Optical anti-counterfeiting with cholesteric liquid crystal emulsions: preparation, properties, and applications

Buchaiah Gollapelli, \* Supraja Potu, Rakeshkumar Rajaboina and Jayalakshmi Vallamkondu \*

Creating sophisticated anti-counterfeiting tags with unique optical characteristics and detailed security attributes is a highly desirable objective to establish a robust authentication capacity across different stimulus modalities. The ability of structured photonic materials to periodically alter their refractive index enables selective diffraction of specific wavelengths and the tuning of optical density states, leading to the discovery of novel optical properties. This fine-tuning is advantageous for numerous optical applications. Using emulsion templates, microparticles with photonic structures have been created, offering enhanced features and functionalities beyond those of standard films. In this realm, cholesteric liquid crystal (LC) emulsions have recently attracted significant interest. Their inherent periodic structures and modifiable optical signals, responsive to external stimuli, present unique benefits and a broad spectrum of applications in optical anti-counterfeiting. This review explores the preparation techniques of cholesteric LC emulsions, the latest developments in cholesteric LC droplets for various anti-counterfeiting intensities, and the range of optical anti-counterfeiting effects achievable with these droplets under different stimulus conditions. It also provides a brief overview of the existing challenges and prospective future applications of cholesteric LC droplets in anti-counterfeiting systems. The aim of this review is to offer fresh insights and suggestions for enhancing optical anti-counterfeiting strategies through the application of cholesteric LC emulsions.

## 1. Introduction

The widespread counterfeiting of trademarks, essential documents like diplomas and certificates, pharmaceuticals, and currency has emerged as a significant challenge in today's world, impacting businesses, government entities, and

Department of Physics, National Institute of Technology Warangal, Telangana, 506004, India. E-mail: [buchaiahg@gmail.com](mailto:buchaiahg@gmail.com), [jayalakshmiv@nitw.ac.in](mailto:jayalakshmiv@nitw.ac.in), [vlakshmij@gmail.com](mailto:vlakshmij@gmail.com)

**Buchaiah Gollapelli**

Buchaiah Gollapelli earned his PhD in soft matter physics from the Department of Physics, National Institute of Technology, Warangal, India. His research work is focusing on soft matter, especially flexible materials with stimuli-responsive properties for sensor and soft actuator applications.

**Supraja Potu**

Supraja Potu received her PhD from the Department of Physics, National Institute of Technology, Warangal, India. Her research work focuses on piezoelectric and triboelectric nanogenerators for self-powered devices and sensor applications.



individuals across various sectors. This issue spans international borders, affecting countries at all stages of development. Counterfeit items include passports, educational and professional certificates, electronic devices, checks, bond certificates, medicines, and currencies, posing risks in multiple domains.<sup>1</sup> With the advancement of science and technology, creating counterfeit items has become relatively easy for fraudsters, prompting researchers to develop robust anti-counterfeiting measures. These efforts focus on creating complex security features using various materials to enhance anti-counterfeiting techniques.<sup>2–6</sup> Among the technologies being explored is the use of radio frequency identification (RFID) with physical unclonable functions (PUF) in electronic anti-counterfeiting strategies. This approach bolsters security by enabling connections with reading devices and servers. Additionally, optical reading techniques like luminous tag technology are widely adopted due to their simplicity, cost-effectiveness, scalability, and ability to convey visual messages. Anti-counterfeiting strategies employing novel fluorescent materials such as organic dyes, lanthanide-based compounds, and carbon dots (CDs) show significant promise.<sup>7–11</sup> Despite their potential, luminescence-based methods face challenges in commercial deployment, including issues like photobleaching, low thermal stability, and matrix-induced luminescence quenching. Current visible authentication techniques include afterglow,<sup>12</sup> up-conversion luminescence,<sup>13</sup> and UV-active photoluminescence, with fluorescent<sup>14,15</sup> patterns being increasingly used for data recording. These patterns are crucial in information security, remaining concealed until activated under specific conditions to reveal encrypted images or data. However, traditional fluorescent designs have limitations, including a restricted image capacity and vulnerability to replication due to their well-documented optical properties. This necessitates the development of scalable, easily verifiable anti-counterfeiting systems using functional materials with unique optical properties. The challenge lies in creating innovative fluorescent patterns capable of displaying multiple designs in response to different

stimuli, allowing for the integration of various images into a single recording space. This advancement would significantly enhance the effectiveness of anti-counterfeiting measures.

Structural color is generated through the interplay of light with a periodic modulation of the refractive index at the nanoscale. This interaction leads to the reflection of a specific wavelength through constructive interference. The dimensions of the periodic nanostructure and the refractive indices of materials determine the wavelength of the reflected light.<sup>16</sup> Various living organisms such as chameleons, butterflies, and beetles, along with human-made materials like anti-counterfeiting labels and iridescent films for decoration, showcase a diverse structural colorations.<sup>17,18</sup> The use of camouflage represents a vital survival tactic adopted by various animal species in their natural environments. To achieve this goal, certain members of the animal kingdom have evolved an extraordinary ability to alter their external features, particularly their color and shape.<sup>19</sup> This adaptation allows them to communicate or blend seamlessly with their surroundings, serving the purpose of self-camouflage.<sup>20,21</sup> The fundamental concepts of coloration, period, anisotropy, and orderliness have ignited innovative design opportunities for advanced devices, smart sensors, and reliable optical encryptions.<sup>18,22</sup> Smart optical materials, with the ability to dynamically adjust their microstructures and optical behaviors in response to external stimuli, distinguish themselves among biomimetic optical materials. This characteristic sets them apart, as they hold potential for a broad spectrum of applications.<sup>23,24</sup> Stimuli-responsive photonic crystals (PCs) with intricate periodic microstructures are highly attractive materials, as they generate structural colors without the need for batteries.<sup>25,26</sup> Cholesteric LCs, a type of stimuli-responsive PC, have garnered significant interest due to their self-assembled helical superstructures and easily fabricated one-dimensional PC structures. The helical pitch of cholesteric LCs can be adjusted to produce vibrant Bragg reflections across the entire visible wavelength range, visible to the naked eye.<sup>27–29</sup> Dynamic fluorescent patterns might be



**Rakeshkumar Rajaboina**

*design and development of various triboelectric nanogenerator devices and their applications in different fields.*

*Rakesh Kumar Rajaboina received his PhD from the Department of Instrumentation and Applied Physics, Indian Institute of Science (IISc) Bangalore, India. He worked as visiting faculty at Department of Physics, IISER-Bhopal in 2015. He is currently working as an Assistant professor at the National Institute of Technology (NIT) Warangal, in the Dept. of Physics from 2018 onwards. His research work is focusing on the*



**Jayalakshmi Vallamkondu**

*the synthesis of 2D Materials, and Liquid crystal-2D material composites.*

*Jayalakshmi Vallamkondu is an Associate Professor at the National Institute of Technology, Warangal, India. She received her doctorate in Physics from Centre for Nano and Soft Matter Sciences, Bangalore, India in 2010 and subsequently pursued post-doctoral research at Queen's University, Canada and Georgia Institute of Technology, USA. Her research interests include soft matter, photodetectors, gas sensors, Geometrical restrictions, Biosensors, Soft Actuators, syn-*



created if fluorescent dyes were used with these cholesteric LC materials. This would be beneficial for various information encryption and anti-counterfeiting applications.<sup>30</sup>

In nature, structural colours are rather common and result from the interaction of light with complex material structure. They are frequently discovered in materials having periodic spatial structures called photonic crystals. Structural colours are regarded as a great alternative to conventional chemical dyes and pigments because of their fading resilience, dynamic adaptability, and non-pollution. Compared to dyes and pigments, structural colours many benefits, such as fading resistance, environmental friendliness, energy efficiency, durability, and high degrees of stability.<sup>31</sup> Additionally, structural colours last longer than dyes and pigments. Even more intriguingly, the colors can be changed by adjusting the helical pitch in response to outside inputs.<sup>32</sup> As a result, a wide range of applications are possible, such as dye-free colour coatings, colour that changes in response to stimuli, colorimetric sensors, and reflective colour displays. Existence of cholesteric structures in biological systems is correlated with their varied functions, which range from the generation of structural colour in insects to the enhancement of the mechanical characteristics of plant cell walls.<sup>27,33</sup> When incident light meets the surface of cholesteric LC, a 1D photonic crystal with a distinctive helical and periodic structure, it displays a vivid reflecting colour. As a result, cholesteric LCs are frequently used in electronic displays, diagnostics, smart clothing, and a number of other applications.<sup>34</sup>

LCs, typically managed in solid film slabs, exhibit intriguing physical phenomena upon confinement within micrometer-sized emulsion droplets.<sup>35</sup> One fascinating illustration pertains to the extraordinary susceptibility of the LC's orientational arrangement in close proximity to interfaces. The exquisite sensitivity of the system enables the propagation of interactions at the molecular scale, manifesting at the interface and permeating throughout the bulk. This phenomenon gives rise to the emergence of unique structures characterized by manipulable topological defects and dislocations. There is an increasing fascination with the utilization of spherical confinements for LCs at interfaces between liquid phases, particularly when these LCs are dispersed in water and adorned with surfactants. Such configurations have paved the way for innovative possibilities in crafting intricate, responsive soft materials. Furthermore, they have facilitated a plethora of unprecedented applications in photonics, sensing, and soft robotics.<sup>36,37</sup> As of now various reviews are reported on anti-counterfeiting using various luminescent materials<sup>2,38</sup> photoluminescent and chromic nanomaterials,<sup>39</sup> cellulose<sup>6</sup> But to the best of our literature knowledge, there exists no such review articles based on anti-counterfeiting using cholesteric LC emulsions.

This review article presents an in-depth analysis of recent progress in the field of structural color encryption and anti-counterfeiting measures using cholesteric LC emulsions. It includes detailed sections outlining the manufacturing process of cholesteric LC emulsions and examines their diverse properties. The article further discusses the methods of optical signal

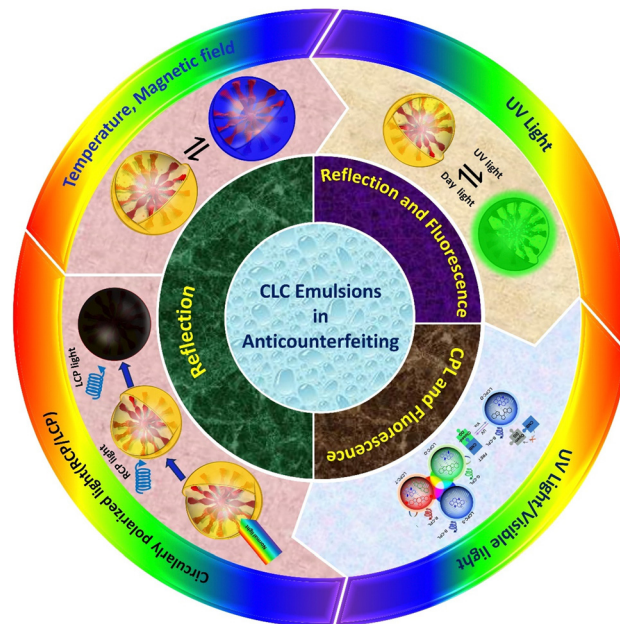


Fig. 1 Schematic showing the outline of this review on optical anti-counterfeiting using cholesteric LC emulsions.

variation in cholesteric LC emulsions for anti-counterfeiting purposes, focusing on the techniques for encrypting and decrypting sensitive information. Towards the end, it addresses the challenges and prospective future directions in employing cholesteric LC emulsions for anti-counterfeiting applications. An illustrative summary of the entire review is provided in Fig. 1, offering a comprehensive visual representation of the covered topics. We anticipate that advanced anti-counterfeiting systems utilizing stimulus-responsive cholesteric LC emulsions will drive research toward elevated levels of information security and the development of more sophisticated anti-counterfeiting technologies.

## 2. Introduction to liquid crystals

LCs represent intriguing soft materials endowed with stimuli-responsive characteristics, where the amalgamation of liquid's mechanical traits and the anisotropic attributes of crystals is observed. These LC molecules, alternatively termed mesogens, exhibit distinctive orientational features and diverse degrees of translational/positional order, while maintaining their inherent liquid fluidity.<sup>40</sup> Typically, LCs can be categorized into two types: thermotropic LCs or lyotropic LCs. The former refers to materials that demonstrate the LC phase within a specific temperature range. The majority of thermotropic LCs consist of organic molecules, characterized by anisotropic shapes reminiscent of rods, discs, and bananas. The term lyotropic LCs pertains to substances that, when dissolved in a particular solvent concentration, display the LC phase. While most LC phases are composed of organic molecules or polymers, inorganic materials like graphene and metal oxide nanosheets can also be dispersed in a solvent to induce an LC phase. The







Fig. 2 (a) Schematic showing the arrangement of molecules in various LC phases. (b) Helical arrangement of cholesteric phase after adding chiral dopant. (c) Schematic representation of director orientation in right-handed and left-handed in helical structure of cholesteric LCs.

arrangement of LC molecules results in various distinct phases, each characterized by specific molecular arrangements and properties. Three primary types of these phases are commonly observed: the nematic phase, the smectic phase, and the cholesteric phase, as illustrated in Fig. 2(a). Within the smectic phase, the self-assembly of LC molecules adopts a layered structure reminiscent of the organization seen in solid crystals. In contrast to the nematic phase, characterized by predominant orientational ordering, the smectic phase displays a dual characteristic with both orientational and positional ordering. In this phase, LC molecules arrange themselves into layers with a specific orientation, resulting in a well-structured and organized configuration. Conversely, the nematic phase is distinguished by exclusive orientational ordering, where the alignment of LC molecules occurs along a specific direction without any accompanying positional ordering. This leads to a more fluidic and less organized state when compared to the structured arrangement found in the smectic phase. The commonly used term for the favored direction of molecular alignment is the director ( $n$ ). When external influences or stimuli are absent, molecules in the nematic phase align along a specific direction, showcasing their orientational order. Chirality significantly influences the physical properties of LCs. The introduction of chirality to LCs leads to the emergence of new mesophases with intriguing physical characteristics. When a chiral molecule is introduced into an achiral nematic matrix,

the cholesteric phase is created, as depicted in the Fig. 2(b). Imparting chirality to the nematic phase allows for the preparation of liquid photonic crystals, where molecules in the cholesteric phase arrange themselves into helical configurations, displaying Bragg reflections.<sup>41</sup> Cholesteric LCs are sought-after materials for photonic surfaces due to their helical structure, serving as a Bragg reflector with a reflection peak dependent on both the average refractive index and the cholesteric pitch. The cholesteric pitch represents the distance over which the molecular director completes one full rotation.<sup>42</sup>

The cholesteric LC phase is characterised by a helical configuration formed by the molecular director as it rotates at regular intervals around an axis. This helical helix's orientation depends on the presence of a chiral dopant. The pitch ( $P$ ) is equal to the distance required by the director to rotate at full  $360^\circ$ . The cholesteric LC material acts as a photonic micro or nanostructure due to the periodicity of the director's rotation, and the reflected wavelength is determined by the following equation:  $\lambda = nP \cos \theta$ , where  $\theta$  is the incident angle,  $n$  is the average refractive index,  $P$  is the pitch, and  $\lambda$  is the reflected wavelength. Cholesteric LCs exhibit some degree of angular dependence with respect to the incident light, manifesting as a blue shift when viewed from an angle that is different from the normal incidence angle. It is possible to alter the structural colour by modifying the pitch, which determines the spectral position of the reflection wavelength. When chiral dopants are



added to cholesteric LC mixtures, the pitch is calculated as follows:  $P = \frac{1}{C \times \text{HTP}}$  where 'C' denotes the concentration and HTP denotes the helical twisting power of the chiral dopant. The HTP of a chiral dopant quantifies its ability to induce a helical twist in a nematic LC host. In cholesteric LC mixtures with a low molar mass, the pitch, and resulting structural colour, can be modified with temperature, electric fields, or light. Due to their fluidic nature, low molar mass cholesteric LCs cannot be further distorted when held between two glass plates. Making a deformable, self-supporting film is feasible by spreading cholesteric LC droplets in a polymer matrix. It is possible to create freestanding films with preserved cholesteric phase by polymerizing cholesteric LC mixtures with reactive monomers (RMs) to create polymer networks. The helical superstructure of the cholesteric LCs allows them to divide iridescent light into two circularly polarized lights that have opposing handedness. On the other hand, they are able to reflect the circularly polarized lights that have the same handedness as themselves while simultaneously transmitting another circularly polarized light as shown in Fig. 2(c).

The capacity of smart optical materials to dynamically alter their microstructures and optical properties in response to environmental stimuli makes them particularly appealing for a variety of applications. Since each mode has several states and permits reversible conversion of those states, designing materials with multi-mode features, such as reflecting colour, fluorescence, and circularly polarized luminescence (CPL) signal, is crucial to obtaining high levels of anti-counterfeiting performance.

Cholesteric LCs can be used to fabricate CPL-active materials with exceptionally high glum. The mechanisms for generating CPL in cholesteric LCs can be broadly categorized into two types.<sup>43,44</sup> The first is optical rotation, where the helical assembly superstructure of cholesteric LCs realizes the chirality amplification effect. In this case, the resulting CPL is transmitted along the helical axis of the cholesteric LC, with its polarized direction following the director twist. The second mechanism is the selective reflection of circularly polarized light, which is employed to achieve strong CPL with high glum. Here, the emission peak is located at the center of the selective reflection band of cholesteric LCs. The cholesteric LCs reflect CPL with the same helical handedness as that of the cholesteric LCs, while CPL with the opposite helical handedness is transmitted through the planar cholesteric LCs cell. Several strategies have been developed to obtain emissive cholesteric LCs, including grafting chiral and luminescent moieties onto LC molecules, and blending chiral dopants and fluorescent dopants into nematic LCs. The introduction of chiral fluorescent dopants, which combine both chirality and fluorescence in a single entity, into nematic LCs appears to be the simplest and most convenient method for constructing emissive cholesteric LCs. Commonly used chiral fluorescent dopants include binaphthyl derivatives and cholesterol derivatives.<sup>45,46</sup> This type of doped emissive cholesteric LC offers several advantages.

The researchers concentrate more on stimuli-responsive substances, particularly light-responsive substances like spiro-pyran diarylethene and azobenzene. Due to external stimuli including heat, radiation, mechanical stress, and electromagnetic field, these stimuli-responsive materials will dynamically alter their reflective colour or fluorescence over time.<sup>47,48</sup> Cholesteric LC droplet dispersion is utilized to create smart materials such as controllable reflective color coatings, programmable lasers, bio- and chemo sensors. The choice to employ a plethora of cholesteric LC droplets is due to the wide variety of orientational structures that were developed. These structures are determined by the boundary conditions, the shape of the droplet, the elastic constants, the size ratio of the droplets, and the cholesteric intrinsic helix pitch.<sup>49</sup>

### 3. Preparation of cholesteric liquid crystal emulsions

Emulsions are a type of colloidal dispersion consisting of two or more immiscible liquids, it can be single, double or multiple emulsions.<sup>50</sup> Single emulsions are the most common type of emulsions and are composed of two immiscible phases where one phase dispersed in the other. They can have more complex structures with multiple phases, and they offer unique properties and applications.<sup>51</sup> Multiple emulsions have a wide range of applications in various industries, including pharmaceuticals, food, and cosmetics, where controlled release of active ingredients or encapsulation is desirable. In complex emulsions, configurations also range from core-shell structures,<sup>52</sup> Janus,<sup>53</sup> or dispersed internal micro-droplets.<sup>54</sup>

LC emulsions are commonly produced using fabrication methods similar to those utilized for isotropic emulsions.<sup>55</sup> One of the methods currently used to prepare emulsions is stirring or vertexing.<sup>56</sup> A particular kind of emulsion where at least one of the phases is an LC is known as a LC emulsion. Emulsions are combinations of two incompatible liquids, like oil and water, that have been stabilised by a surfactant. Stirring and vertexing are quick and affordable methods for creating LC emulsions in comparison to other methods. These techniques entail mechanically splitting the bulk LC into minute droplets, which presents challenges in terms of regulating the size and attaining homogeneity (Fig. 3(a)). Besides, ultrasonication is another common alternative for preparing the LC emulsions in which pressure waves at ultrasonic frequencies induce a strong oscillating shear flow (Fig. 3(b)). In the form of a miniemulsion, this method can make droplets that are smaller than the micron scale and have a slightly narrower size range. Even ultrasonication, which aims for size uniformity, fails to produce monodisperse droplets.

Microfluidic emulsification has emerged as a method to obtain significant control of size, shapes, and compartments of emulsions.<sup>54,57</sup> It involves the processing and attempting to manipulate the fluids passing through channels with sizes ranging from tens to hundreds of micrometres. In its simplest form, the dispersed phase is forced into the continuous phase





Fig. 3 Schematics depicting the production process of LC emulsions: emulsification through (a) stirring, (b) ultrasonication represent bulk emulsification strategies. Microfluidic emulsification using (c) PDMS cross-junction microchannel, while (d)–(g) involve microfluidic emulsification using a tip-to-tip microchannel, enabling the fabrication of single emulsion (d) and (e), double emulsion (f), and triple emulsion (g), respectively. (h) Suspension (top) and precipitate polymerization (bottom).

through tiny channels, to generate monodisperse emulsions shown in Fig. 3(c)–(g). Sequential capillary junctions allow access to multi-compartment emulsions, from double, to triple, to more complex structures.<sup>58</sup> Unlike conventional emulsification methods, the double and triple emulsions produced by microfluidics can be perfect core-shell. Although the configuration and composition (*e.g.*, double, triple) of the emulsions is determined by the geometry of the capillary devices, the size of the emulsions can largely be controlled by the capillary diameter and flow rate of each phase, with additional considerations such as fluid viscosity and other fluid properties.<sup>59</sup> Finally, successful fabrication also relies on adjusting the wetting properties of the capillary channel. Microfluidic emulsification not only gives significant control over the structure and size of emulsions, but it also has a higher emulsification efficiency (decreased volumes of solvents and surfactants) than conventional methods; however, microfluidic emulsification has limitations on the minimum size of emulsions produced (generally  $> 10 \mu\text{m}$ ) and lower throughput.<sup>60</sup>

The use of soft lithography techniques developed by Whiteside's group enabled the remarkable development of microfluidics.<sup>61,62</sup> Due to its low cost, ease of functionality, gas permeability, and excellent transparency, PDMS is the most frequent element used in constructing devices for microfluidics systems. Soft lithography cross-junctions (Fig. 3(c)) can be used to prepare LC emulsions. In the cross-junction geometry, LC droplet formation occurs as water flows through the main channel as the continuous phase, while LCs are injected through the lateral channel as the dispersed phase. The LC-water interface forms at the cross-junction, where the pressure gradient distorts the LCs into droplets. Finally, the LC-in-water emulsion is assembled in the channel. Although PDMS casting

is a simple and commonly used method for fabricating microfluidic systems, adjusting its surface to be sufficiently hydrophilic remains a major challenge. Hydrophilic channels are necessary for oil in water emulsions to prevent the dispersed phase from adhering to the walls. An entirely different approach for the fabrication of microfluidic devices using glass capillaries on a glass slide was introduced by David A. Weitz group in 2007.<sup>45</sup> In capillary microfluidics, the simplest axisymmetric geometry is the co-flow setup (Fig. 3(d)), where LC flow inside the inner capillary and water flows through the outer capillary in the same direction, forming individual monodisperse LC droplets at the tip of the inner capillary.<sup>59</sup> As can be seen in Fig. 3(e), in contrast to co-flow capillary devices, an additional symmetrical capillary positioned oppositely with the original inner capillary, is introduced to create a flow-focusing effect that aids in producing stable droplets.<sup>63</sup> Instabilities in the LC phase, driven by Rayleigh instability, lead to the formation of droplets at the interface between two immiscible phases, with amphiphilic molecules adhering to their surfaces. Increasing surface coverage by these molecules in aqueous solution prevents droplet coalescence. This intricate process is influenced by flow conditions, interfacial tension, viscous forces, and channel geometry. Moreover, optimizing the channel wall surface for efficient wetting by the continuous phase promotes the stable development of LC droplets. In addition to forming single LC emulsions, where LC is confined within spherical droplets dispersed in a liquid medium, these techniques also facilitate the creation of complex multi-compartment emulsion droplets. These droplets demonstrate precisely defined volumes and compositions, showcasing a diverse array of structures such as water-in-LC-in-water (W/LC/W) shells, Janus emulsions, LC-in-fluorocarbon-in-water (LC/F/W), and





fluorocarbon-in-LC-in-water (F/LC/W), among other configurations. By combining co-flow and flow-focusing geometries in coaxial flow-focusing glass microcapillary devices, droplets of LC double emulsion droplets can be produced, where the LC phase serves as the emulsifier.<sup>63,64</sup> The inner fluid is an aqueous solution, which is injected through a cylindrical injection capillary (Fig. 3(f)). The middle fluid, LC, is injected through the spaces between the cylindrical and square injection capillaries. Because of capillary instability, water-in-(W/LC) emulsions form at the left inner capillary's tip as the LCs partition the inner aqueous phase. As these drops encounter the aqueous continuous phase, which is moving in the opposite direction, they combine to produce W/LC/W double emulsion droplets in which LCs occupy the middle layer.<sup>65–67</sup> Using microfluidics, it is possible to produce triple emulsions using a three coaxially aligned capillary device as shown in Fig. 3(g).

Classical polymerization techniques, illustrated in Fig. 3(h), present alternative methods for generating LC droplets with diminished sizes ( $<10\ \mu\text{m}$ ).<sup>68</sup> Among these approaches, precipitation polymerization is notably intriguing, enabling the creation of nearly monodisperse LC polymer droplets with diameters of approximately  $\approx 1\ \mu\text{m}$ .<sup>69</sup> Initiating with a uniform solution of reactive LC monomers, the process unfolds with polymerization. This results in the precipitation of newly formed polymer chains, leading to the creation of initial particles that grow and eventually form the final LC particles. In contrast, suspension and mini-emulsion polymerization entail dispersing a blend of LC monomers in the continuous phase through bulk emulsification, followed by the polymerization process. Both methods are adaptable to a wide range of LC phases, providing flexibility in producing LC polymer particles with diverse size distributions. Suspension polymerization yields average diameters surpassing  $1\ \mu\text{m}$ , whereas mini-emulsion polymerization attains average diameters below  $1\ \mu\text{m}$ .

## 4. Properties of cholesteric liquid crystal emulsions

The use of microdroplets not only facilitates the exploration of the fundamental self-assembly behavior of cholesteric LC molecules but also enables the study of their characteristics under conditions of spherical confinement. This controlled environment reveals observations of molecular alignment along the boundary. Because of their natural insolubility in water, LC phases are frequently used to create oil-in-water (O/W) emulsion droplets through the methods explored in Section 3. These methods are employed to generate photonic droplets and microspheres. While the orientation of LC molecules during emulsification may initially be entirely random, throughout the formation of the spherical emulsion droplet, they eventually align to establish a specific orientation with the surfactants.

The nematic LC phase, characterized by mesogens exhibiting solely orientational order, has been extensively employed in

droplets. Within this phase, mesogens can align either parallel (planar) or perpendicular (homeotropic) to the interface, resulting in bipolar or radial configurations, respectively.<sup>70,71</sup> As an example, surfactants with lengthy alkyl chains orient their hydrophobic alkyl chains perpendicular to the LC water interface. This arrangement causes mesogens to align in a homeotropic manner, resulting in a radial configuration. Surfactants like sodium dodecyl sulfate (SDS), hexadecyltrimethylammonium bromide (CTAB), and polysorbate-type surfactants (Tween) are examples. However, polymeric surfactants, including polyvinyl alcohol (PVA) or polyvinylpyrrolidone (PVP), exhibit absorption at the LC water interface in a random coil conformation. This results in the alignment of mesogens parallel to the aqueous interface and the generation of a bipolar configuration.<sup>27</sup>

As we know infusing chirality into a nematic LC phase causes a rotation in the mesophase director, giving rise to chiral nematic LCs, commonly referred to as cholesteric LCs (refer to Fig. 2(b)). These cholesteric LCs have been widely applied in the fabrication of cholesteric LC droplets, capitalizing on their characterization as one-dimensional photonic materials that reflect light due to their periodic helical formation. It is imperative to meticulously manage anchoring conditions at interfaces to ensure the production of cholesteric LC droplets with precisely delineated internal helical configurations. In the presence of PVA, cholesteric LC molecules exhibit a preferential tangential orientation at the LC water interface, resulting in the development of a radially aligned helical cholesteric LC phase. This planar alignment imparts a unique visual appearance to cholesteric LC droplets, as depicted in Fig. 4(a). By employing the technique of polarised optical microscopy (POM), one can effectively demonstrate the manifestation of the Maltese cross pattern as well as a series of concentric circles. Cholesteric LC emulsions, apart from manifesting a photonic stopband, showcase a wide variety of colors when observed through the lenses of unaided or aided POM. The centre wavelength of the reflected light is determined by the incident angle and the properties of the cholesteric LC core. Due to the selective reflection of circularly polarised light, cholesteric LC droplets exhibit a coloured dot on their upper or top surface when exposed to unpolarized white light. Furthermore, when the droplets are placed close together, additional optical patterns arise in the peripheral of each droplet *via* photonic cross-communication.<sup>72,73</sup>

Conversely, in the presence of SDS within the continuous phase, the cholesteric LC molecules within the droplet orient themselves perpendicular to the interface. This results in irregular patterns of fractured color spots on the surfaces of the droplets, as depicted in second row of Fig. 4(a). In essence, the anchoring condition, which can be dynamically altered by the adsorption and removal of surfactants with alignment preferences, is the decisive factor determining the optical patterns of cholesteric LC droplets.<sup>74,76</sup> The photonic stopband can also be tuned by manipulating temperature, magnetic field, and electric field. Increasing the temperature can have opposing effects on the pitch: one way it does this is by increasing the



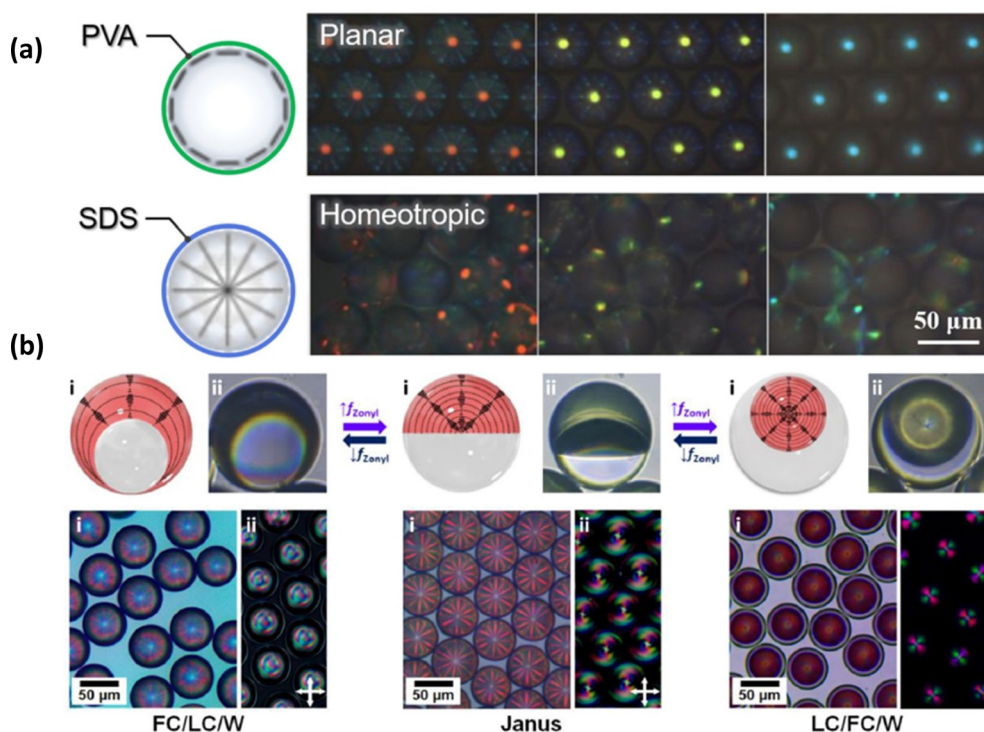


Fig. 4 (a) Cholesteric LC droplets exhibiting planar and homeotropic configuration. Adapted from ref. 74 with permission. Copyright©2016 American Chemical Society. (b) Complex LC emulsions exhibiting dynamic reconfiguration in response to variations in surfactant content between F/LC/W double emulsions, Janus droplets, and LC/F/W double emulsions. Adapted with permission from ref. 75.

solubility of the chiral reagent, which can have the effect of lowering the pitch, and another way is by speeding up the phase transition, which can raise the pitch. An intriguing characteristic of the photonic stopband pertains to its selectivity regarding the handedness of the incident circularly polarised light. Specifically, the cholesteric LC of LH type core exclusively reflects left circularly polarised light, whereas the RH cholesteric LC core exclusively reflects right circularly polarised light.

Cholesteric LC double-emulsions, distinguished by the nesting of inner drops within outer drops to form a core-shell geometry, can be produced under precise control using microfluidic technology, whether a two-step or single-step emulsification process is used. Because of their insolubility in water, LC phases can be used with either a W/LC/W or LC/W/LC composition. The former is predominantly showcased and applied in various applications. Cholesteric LC shells are produced through the utilization of W/LC/W double-emulsion droplets. This arrangement, with the cholesteric LC sandwiched between two aqueous interfaces, results in greater alignment and subsequently higher optical performance compared to single-emulsion droplets of cholesteric LC. As the thickness of the shell decreases, reflection colour patterns caused by direct reflection and photonic cross-communication become more distinct for planar alignments at both interfaces, even though the number of layers contributing to the stopband decreases.<sup>62</sup>

Swager and colleagues reported on the creation of complex emulsions involving immiscible nematic LCs and fluorocarbon

oils. The incorporation of an additional interface introduces additional topological constraints, which can be finely controlled using specially designed surfactants to ensure specific anchoring of the mesogens at each interface. This approach led to the preparation of complex LC emulsions with diverse internal configurations, allowing for the transformation between double emulsions LC/F/W, Janus emulsions, and F/LC/W double emulsions. The versatility extended to the use of both smectic and cholesteric phases, resulting in complex LC emulsions with intricate internal arrangements as shown in the Fig. 4(b).<sup>75,77</sup> Furthermore, employing polymerization techniques enabled the generation of non-spherical structures with complex internal LC organizations.

The utilization of multiple emulsion droplets of elevated order has been implemented as a tactic to tackle the constraints linked with double emulsions. The utilization of oil-in-water-in-oil-in-water (O/W/O/W) triple-emulsion droplets has been observed to generate cholesteric LC microcapsules that demonstrate superior molecular alignment and mechanical characteristics in comparison to microcapsules that are templated by O/W/O double emulsions.<sup>52,78</sup>

## 5. Application of cholesteric liquid crystal emulsions in anti-counterfeiting

Contrary to conventional labels that enhance the aesthetic appeal of products, anti-counterfeiting labels are intended to





minimise economic damage caused by counterfeiting. The cutting edge of next-generation anti-counterfeiting technology is security inks, which can transfer personal information *via* a variety of optical states. The unusual optical appearances of cholesteric LC droplets or cholesteric LC droplet arrays are due to their geometry and cannot be developed in a conventional film format.<sup>73</sup> As previously stated, arrays of cholesteric LC droplets exhibit photonic cross-communication-induced colour patterns on the side surface in addition to the strong reflection dot on the uppermost region. Emulsions containing cholesteric LC phases showcase outstanding photonic characteristics, including circularly polarized reflection and omnidirectional lasing. Cholesteric LC emulsions have the ability to alter their optical features based on external environmental changes or through the introduction of fluorescent substances, imparting fluorescent properties to the cholesteric LC emulsions. These attributes can be employed to encode crucial information into distinct color signals, allowing the cholesteric LC emulsions to identify and interpret these signals. Consequently, functionalities such as anti-counterfeiting and information encryption can be achieved, enhancing the security and confidentiality of information.

### 5.1 Using reflection properties

Cholesteric LC emulsions have found application in anti-counterfeiting inks in recent years due to their distinct optical features, in particular the polarization-dependent reflection made possible by the photonic stopband.<sup>79</sup> As mentioned earlier, it has been observed that arrays of cholesteric LC droplets exhibit colour patterns on their side surfaces due to photonic cross-communication, in addition to the presence of a concentrated reflection dot in the uppermost region. Retroreflection paths are established to facilitate double reflections by a pair of droplets, irrespective of the prevailing conditions of the medium. This phenomenon gives rise to the formation of

blue-shifted colour dots or lines, the quantity of which is directly proportional to the number of pairs. It is worth noting that while the angles of light incidence and reflection ideally measure  $45^\circ$  for a perfectly planar wave, deviations can occur due to the numerical aperture of the lens employed in the optical microscope.

In addition, it is possible to induce the polymerization of cholesteric LC droplets, leading to the formation of solid microspheres, through the utilization of a RM. Solidification enhances LC droplets' mechanical stability, simplifying post-processing procedures and broadening the scope of potential applications. The process of photopolymerization of RMs results in the conversion of fluidic cholesteric LC droplets into solid spheres, while maintaining the molecular alignment of the LC. An alternative approach to stabilise cholesteric LC droplets involves the encapsulation of these droplets within a polymer shell. This can be achieved through interfacial polymerization or coacervation of precursors at the surface of the cholesteric LC droplets. The polymer shell exhibits a sufficiently thin structure that allows for the observation of inherent optical patterns, while simultaneously maintaining a high level of mechanical durability.<sup>80,81</sup>

Cholesteric LC droplets can be further designed to allow active colour switching by varying the handedness of the circular polarisation (Fig. 5(a)). Cholesteric LCs can exhibit a stopband for circularly polarised light with the same handedness as their helical structures. The chiral dopant determines whether the photonic cholesteric LC reflects right-handed (RH) or left-handed (LH) circularly polarised light. A RH (or LH) chiral dopant and a nematic LC can be mixed together to make a RH (or LH) twisted helical structure. So, the cholesteric LC only reflects circularly polarised light with the same handedness, and the Bragg relationship governs the wavelength of the reflected light. Photonic films containing a secret message can be made by combining RH and LH-cholesteric LCs with a

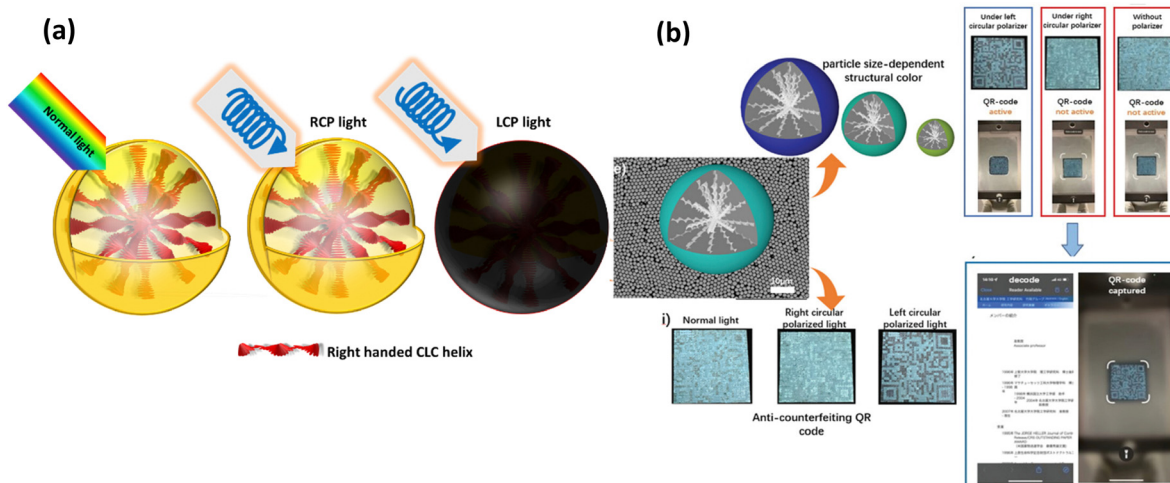


**Fig. 5** (a) Principle of anticounterfeiting using polarized light in cholesteric LC droplets (b) Particle sizes dependence of the structural color of cholesteric LCs particles. Photographs of cholesteric LCs particle-based anti-counterfeit QR code under normal light, right-, and left-circularly polarized light. The anti-counterfeiting QR code was captured and decoded by a smartphone under the left circular polarizer and linked to the home page of the Takeoka group. Reproduced with permission.<sup>83</sup> Copyright 2023, John Wiley and Sons.



patterned structure. Enriching their uses for anti-counterfeiting, in particular, is the patterning done at the selected section, which features varied handedness. As a result, one can develop new interactive materials by combining two cholesteric LCs with opposing handedness. Based on this idea, in 2013, Guo *et al.* used interfacial polymerization to make a cholesteric LC microcapsules film with a doublehanded circularly polarised light reflection band. Cholesteric LC microcapsules with both right-handed and left-handed structures are mixed together and coated on a glass substrate to make cholesteric LC films with a double-handed structure. The produced cholesteric LC-M film has temperature-dependent light-reflection characteristics. Because of the pitch length asymmetry between the left- and right-handed cholesteric LCs, two distinct reflection bands may be seen at 25 °C. At 45 °C, however, due to a shift in pitch length, both left circularly polarized and right circularly polarized lights are reflected in the same reflection band.<sup>82</sup>

Seo *et al.*<sup>84</sup> generated solid-state cholesteric LC microcapsules by utilizing microfluidic device to construct anti-counterfeiting patches by photopolymerizing RMs RM257 in cholesteric LC droplets. A 3D rigid network is formed by curing RMs for the cholesteric LC microcapsules, which results in an appropriate standard of mechanical stability. Depending on the stable cholesteric LC microcapsules, an anti-counterfeiting patch was developed *via* the combination of two distinct cholesteric LC microcapsules with the same reflection colours but opposing handedness, which displays different letters under different circularly polarised light sources. The utilisation of O/W/O/W triple-emulsion droplets enables the integration of two distinct cholesteric LC phases possessing opposite handedness within a singular microcapsule.<sup>78</sup> When exposed to unpolarized light, the cholesteric LC microcapsules show a colour combination of the two cholesteric LCs in the core and shell; but, when exposed to circularly polarised light, the microcapsules show a preference for either the core or shell colour, depending on the handedness choice. In 2017, microcapsules were prepared using cholesteric LCs of opposite chirality as the core and shell, employing chiral dopants R5011(RH) and S5011(LH), respectively.<sup>52</sup> The ultimate color of the cholesteric LC microcapsules resulted from the combination of the inner and outer shell cholesteric LC colors. Due to the distinct chirality of the core and shell cholesteric LCs, the cholesteric LC microcapsules could exhibit either the color of the core or the shell when observed under different polarizations of light with varying chirality. Therefore, codes can be concealed in patterns made up of arrays of two different microspheres, and revealed with the use of circularly polarized light. He *et al.*<sup>83</sup> synthesized monodisperse cholesteric LC particles through dispersion polymerization (Fig. 5(b)). By forming cholesteric LCs into micrometer-sized monodisperse spheres, they could adjust the pitch of the cholesteric LCs based on particle size, enabling control over the structural color of the cholesteric LC particles by influencing the Bragg reflection spacing and photonic bandgap. This structure can display different structural colors under various circularly polarized lights. Moreover, they developed a straightforward

method to produce chiral anti-counterfeiting QR codes. By integrating cholesteric LC particles with commercially available pigments, they created an anti-counterfeiting QR code that is visible only under a specific circular polarizer.

Yang *et al.*<sup>85</sup> employed *in situ* polymerization with cellulose nano crystal (CNC)-stabilized pickering emulsion as a template to manufacture cholesteric LC microcapsules with CNC and a melamine-formaldehyde (MF) resin hybrid shell. In order to create a thermochromic coating, cholesteric LC microcapsules and a curable adhesive were combined. The thermochromic paint film was found to exhibit colour-changing properties over the visible light spectrum and between a temperature range of 12 and 42 °C (Fig. 6(a) and (b)). The resulting thermochromic paint layer additionally shown a high reflectivity of up to 30–40%.

In addition, the photonic cross-communication property of cholesteric LC microcapsules has been leveraged to implement anti-counterfeiting, demonstrating the benefits of being easy-to-read and impossible to replicate.<sup>73</sup> Photonic cross-communication between cholesteric LC microcapsules is seen to be the best possibility for realising a PUF because of their distinctive optical properties and inherent randomness. Using microfluidic technology and a subsequent UV-curing procedure, Geng *et al.*<sup>86</sup> created microcapsules with a cholesteric LC shell. It is emphasised that the optical quality of traditional cholesteric LC droplets is still not good enough, which severely limits their practical applications. These colour patterns, brought about by photonic cross-communication and multiple internal reflections, are nearly unclonable and can provide high authenticity. However, the aforementioned issue is resolved by a transition from droplet to shell (double emulsion), which guarantees a sharp pattern and high optical quality. Moreover, the security level is improved by merging cholesteric LC shells of varying pitch, thickness, and chirality, as this provides the system with tremendous variation options. For the implementation of future high-security authentication and identification protocols, such a PUF formed from photonic cross-communication is seen as a promising element.

Incorporating functional nanomaterials into photonic structures allows for new and exciting applications for photonic crystals. This strategy can increase the proportion of responsive substances in the system and improve the responsiveness. The researchers Yu *et al.*,<sup>87</sup> created Janus microdroplets using Fe<sub>3</sub>O<sub>4</sub> magnetic nanoparticles doped cholesteric LCs and silicone oil. These microdroplets phase separated when their cosolvent dichloromethane (DCM) was withdrawn. Upon observation from the perspective of the silicone oil interface, it has been observed that cholesteric LCs exhibit a reflective coloration that possesses a 14-fold increase in reflection area as compared to that of homogeneous cholesteric LC spherical microdroplets. The observed rise in values can be ascribed to the phenomenon of internal reflection occurring at the curved interface between cholesteric LC and silicone oil. The fact that silicone oil is lighter than cholesteric LCs causes the Janus microdroplet to constantly orient itself with the silicone oil side up vertically. This causes the colour to self-recover when the particle's



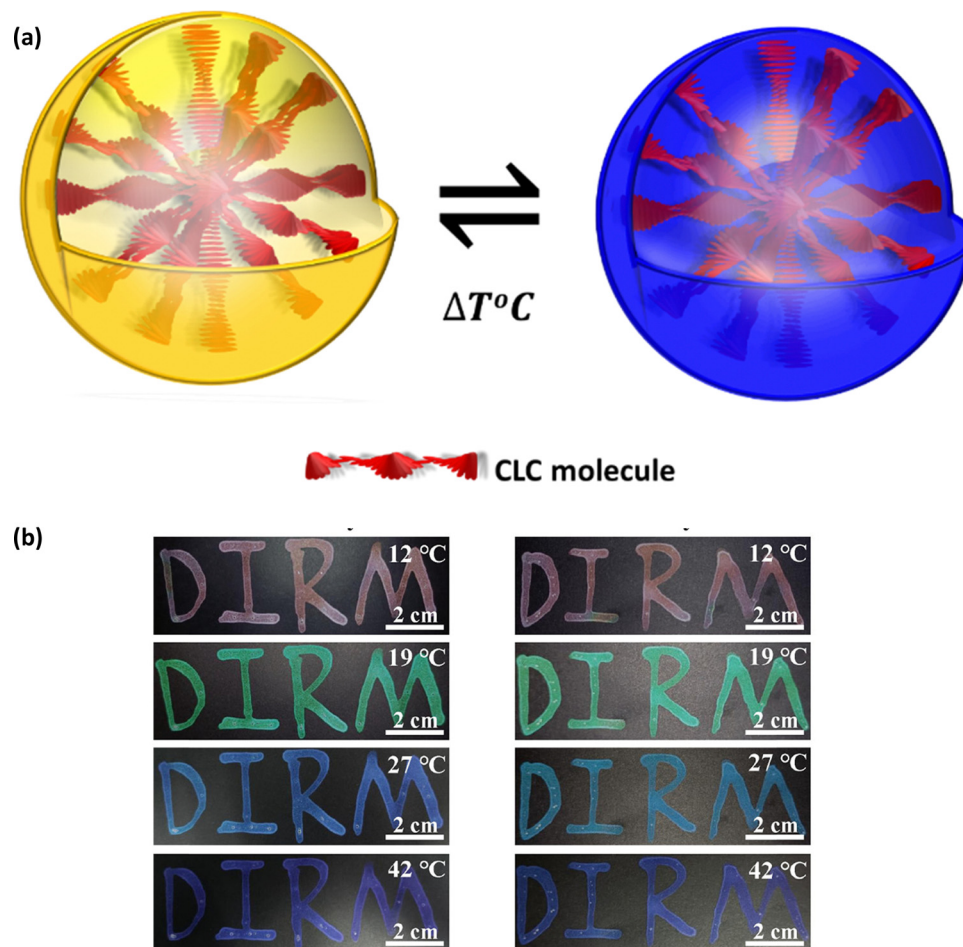


Fig. 6 (a) Principle of anticounterfeiting using temperature as stimuli (b) thermochromic coatings of cholesteric LC microcapsules with cellulose nanocrystals (CNC) and a melamine-formaldehyde (MF) resin hybrid shell with and without dye. Adapted from ref. 85 with permission. Copyright©2022 American Chemical Society.

orientation is altered. They employed magnetic nanoparticles to regulate the orientation of the microdroplets, and as a result, the colours that were exhibited. This allowed the colour displays to be turned on and off by an untethered magnetic field without causing the droplets to become deformed. By combining active and passive Janus microdroplets, they demonstrated the feasibility of data encryption in a variety of configurations. They created a 15-pixel label programming that includes the reflecting structure colour and magnetic responsiveness of the Janus droplets in each pixel individually. The labels may display various encodings depending on the position of the filling. For example, labels display only the structural colors and reveal the letter P when magnetic field was switched ON. Similarly, the number 8 with the same structural color and reveals number 5 in the presence of a magnetic field. These labels show a random design in the initial state, and when the magnetic field is turned on, it reveals the letter Y or number 3 in the pattern based on the pixel filling positions. This method of employing the magnetic field allows the encrypted data to be programmed by each pixel's initial colour and magnetic responsiveness, proving to be a successful method for data

encryption applications in switchable colour displays and counterfeit prevention.

## 5.2 Using fluorescence properties

Luminescent cholesteric LCs have emerged as promising candidates for generating adaptable CPL with significant luminescence dissymmetry factors ( $g_{lum}$ ). This capability is attributed to the inherent self-organized helical superstructure and the responsive nature of cholesteric LCs. A recent advancement involves the creation of a laser array that can manipulate wavelengths and produce CPL through the use of thermosensitive cholesteric LCs. This array was utilized for the encryption of dual-dimensional information based on wavelength and polarization.<sup>88</sup> Furthermore, a multidimensional security label was devised, employing a photochemical dual-responsive CPL material with distinctive wavelength, intensity, and chirality features for information encoding purposes.<sup>89,90</sup> Therefore, the development of phototunable cholesteric LCs systems exhibiting fluorochromic properties and excellent processing performance is strongly desirable. Li *et al.*<sup>91</sup> fabricated solid films suitable for devices by employing LC photonic capsules (LCPCs)







Fig. 7 (a) The light-induced Förster resonance energy transfer (FRET) mechanisms in diverse LCPC components serve as foundational elements for constructing photo-adjustable full-color CPL. (b) The key concept involves designing a 4D information encryption framework, encompassing fluorescence, temporal responsiveness, full-color representation, and CPL attributes. Adapted from ref. 91 Copyright©2023 Springer.

created through interfacial polymerization and adjustable full-color circularly polarized luminescent materials. These materials possessed fluorescence, CPL, full-color emission, and time-responsive characteristics, demonstrating significant advantages in the realm of information encryption. A set of six LCPC

films was utilized to create high-security bar codes that transitioned from initial 1D blue fluorescent codes to 4D full-color circularly polarized luminescent codes with increasing irradiation time. This process showcased the encryption and decryption of 4D information (Fig. 7).



Fig. 8 Schematic depicting the mechanism of anticounterfeiting labels, designed by incorporating fluorescent additives into cholesteric LC droplets.



### 5.3 Using reflection and fluorescence properties

However, cholesteric LC systems with just one structural colour are not the best for meeting the demands of actual applications because of the escalating performance needs of novel materials and the complexities of their environments of usage. Consumers anticipate the appearance of cholesteric LC materials with vibrant colors and a range of uses. Fluorescence is an effective and frequently utilized anti-counterfeiting technology. The invisible fluorescence pattern, which is encoded without stimulation and disclosed under specified circumstances, provides an inherent advantage in information encryption and anti-counterfeiting. One promising strategy for expanding LC applications is by introducing fluorescence into cholesteric LC systems, resulting in fluorescent cholesteric LCs (FCLC) with dual fluorescence and structural colors. Cholesteric LC droplets containing a luminous dye can be used to encrypt information. The droplets exhibit structural colors in white light, but, under UV light, they exhibit fluorescence. It is possible to produce two unique cholesteric LC drops that have the same structural colours both with and without the dye because the fluorescent

dyes do not alter the stopband of the cholesteric LCs (Fig. 8). This is made possible by the fact that the fluorescent dyes do not affect the cholesteric LCs.

Qin *et al.*<sup>92</sup> recently described a method for patterning geminate labels ink using the flow-focusing glass capillary microfluidic technology, which can produce a pattern with two types of entirely different yet intact information. This was achieved by programming luminous cholesteric LC microdroplets (two-tone inks), in which the luminescent material (cyano-substituted oligo (*p*-phenylenevinylene) derivative, DC5) was “coated” with structural colour from helical superstructures. Utilizing the properties of cholesteric LC microdroplets, various microdroplets were introduced into the pixel arrays. This resulted in the presentation of a colourful “Christmas tree” in reflective mode under white light and a gemstone “anti-counterfeit tag” in fluorescent mode featuring a cyan 2D code with decrypted “LC” letters (Fig. 9(a)). In a recent article, we have described how fluorescent carbon quantum dots were added to LC droplets to create fluorescent cholesteric droplets.<sup>93</sup> These fluorescent cholesteric LC droplets showed

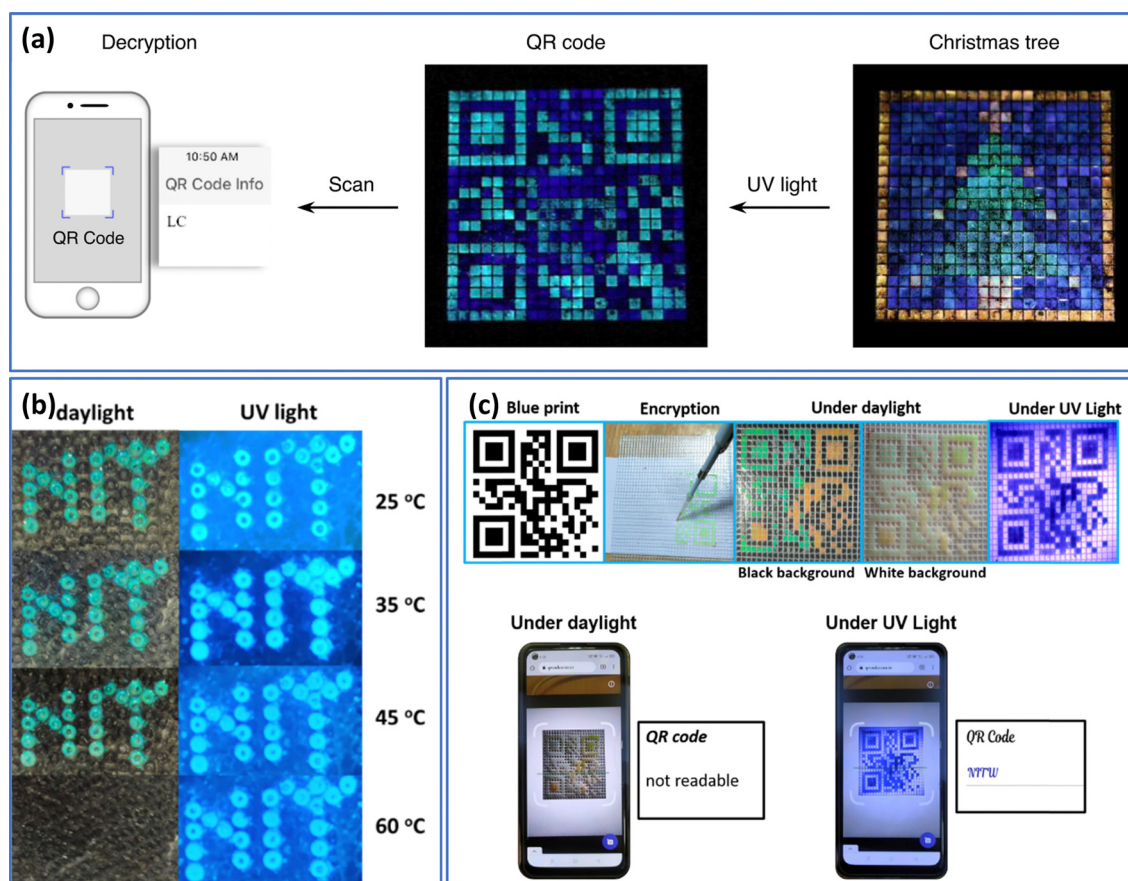


**Fig. 9** (a) The fluorescent QR code representing “LC” is hidden behind a lively reflective “Christmas tree,” revealing its contents through decryption when exposed to UV irradiation ( $\lambda = 388$  nm). Adapted from ref. 92 with permission. Copyright©2021 Springer. (b) Security labels made of Carbon quantum dots doped cholesteric LC droplets displaying the letters “NITW” in structural color under daylight and exhibiting fluorescent colors under UV light. Adapted from ref. 94 with permission. Copyright©2022 American Chemical Society. (c) The method of designing a QR code utilizing chlorophyll dye doped cholesteric LC droplets. Smartphones equipped with QR scanning applications can decipher the encoded message “NITW” from the QR codes under UV light conditions ( $365$  nm,  $10$  mW cm<sup>-2</sup>), making them unreadable in daylight. Adapted from ref. 93 with permission. Copyright©2022 Elsevier.

structural reflection colour in the daylight and fluorescent colour when exposed to UV radiation. Here, in line with study of Qin *et al.*, the fluorescent cholesteric LC droplets stabilized in planar anchoring conditions with displaying the photonic cross communication. However, because to the agglomeration of CQDs in cholesteric LCs, the emission intensity is not up to par. A dual-mode display label was created through the incorporation of fluorescent cholesteric LC films and fluorescent cholesteric LC microdroplets showing “NITW” letters (Fig. 9(b)).

In the subsequent work, we introduced chlorophyll dye to the cholesteric LC to increase the fluorescent intensity.<sup>94</sup> The spinach leaves were used to extract the chlorophyll dye. However, the produced chlorophyll doped cholesteric LC droplets are unstable and showed flashing spots even in the presence of 1–10 wt% PVA. This indicates the doped chlorophyll dye stabilizing the cholesteric LC droplets in homeotropic configuration. They have employed 1–10 wt% Tween 80 as the continuous phase to stabilize the droplets. These fluorescent cholesteric LC droplets showed red, green, and blue (RGB) colours throughout the day and fluorescent colours when exposed to UV light. This mechanism was used to develop authenticated and unauthenticated QR codes and written security labels. A dual-mode display label was created through the incorporation of fluorescent CLC films and fluorescent cholesteric LC microdroplets. The successful demonstration of authenticated/protected QR codes introduces innovative possibilities for anti-counterfeiting labels (Fig. 9(c)). Such two-tone inks showed significant potential in anti-counterfeiting technology as a platform for encrypting and safeguarding vital authentic information.

In a recent study conducted by Chaofeg *et al.*<sup>95</sup> a novel three-state programmed label was introduced by using dye doped cholesteric LC microspheres. The utilisation of the selective reflection principle of cholesteric LC and the

photoisomerization principle of spiropyran (SP) was employed by the researchers in order to devise a novel three-state anti-counterfeiting system. This label possesses the ability to convey distinct information in three distinct states: visible light, UV light, and the absence of UV light. The primary applications of this label include anti-counterfeiting measures and encryption purposes. The researchers employed the selective reflection principle of cholesteric LC and the photoisomerization principle of spiropyran (SP) to develop a three-state anti-counterfeiting system. When comparing the three-state ink with simpler single-state (reflection/fluorescence) and dual-state (reflection and fluorescence) anti-counterfeiting methods, it becomes evident that the former possesses significant potential in the realms of anti-counterfeiting and encryption due to the possibility of one more state which occurs after the removal of UV light and involves the three-state ink displaying a combination of the cholesteric LC structural colour and the colour of the merocyanine (MC) dye. Table 1 lists the different liquid crystal materials used in the anti-counterfeiting technology.

It is worth noting that prior biomimetic optical materials typically exhibit responsiveness to a singular stimulus. The occurrence of multiple stimuli-response in biomimetic optical materials is infrequently documented. Numerous optical materials that are responsive to multiple stimuli have the capability to incorporate diverse mechanisms of stimuli responsiveness, including but not limited to photoluminescence, thermochromism, mechanoluminescence, and electroluminescence. These materials can be utilised to create novel hybrid optical structures or composite optical structures. Moreover, the current challenge lies in developing multiple stimuli-responsive optical materials for hybrid architectures and achieving tunable properties. There is a pressing need for a universally applicable and highly manageable method. In addition, it is possible to fabricate a thermotropic reflection evolution, temperature-

**Table 1** Cholesteric LC emulsions/microcapsules used in anti-counterfeiting technology

S. no.	Material	Stabilizer	Anti-counterfeiting principle	Ref.
1	Left- and right-handed helical structure cholesteric LC mixture	Polyurethane shell composed from isophorone diisocyanate	Both L-circularly polarized light and R-circularly polarized light are reflected by the cholesteric LCs	82
2	Cured cholesteric LC	Water-glycerol, PVA	The photonic cross communication between cholesteric LC microspheres creates a lit PUF	86
3	Janus emulsions of cholesteric LC (composed of non-reactive mesogen 5CB, reactive mesogen RM257 and chiral dopant) and silicone oil	PVA	The display exhibits uniform color and shows letters or numbers when the magnetic field is applied.	87
4	5CB LC based cholesteric mixture	PVA	The phototunable CPL and time-response features were used to encode and decode 4D information.	91
5	DC5 doped cholesteric LC (E7 and chiral dopant)	PVA	The label displays distinct patterns in reflection and fluorescent modes.	92
6	Chlorophyll dye doped cholesteric LC (E7 and chiral dopant)	Tween-80	The label displays distinct colours in reflection and fluorescent modes.	93
7	Carbon quantum dots doped cholesteric LC (E7 and chiral dopant)	PVA	The label displays distinct colours in reflection and fluorescent modes.	94
8	Spiropyran (SP) doped cholesteric LC (E7 and chiral dopant)	PVA	The label displays distinct colours in reflection, fluorescent modes, and removal of UV light	95
9	RECs doped with cholesteric LC (E7 and chiral dopant)	Polyurethane shell composed from TDI and TEPA	The cholesteric LC integrates electro optical response, fluorescent mode, and reflection mode	96





dependent fluorescence emission, and Fredericks electro-optical response in a fluorescent LC microcapsule (FLCMs) by incorporating rare-earth complexes (RECs) into cholesteric LCs. The interaction between the aromatic rings on the RECs and the chiral LC results in a strong  $\pi$ - $\pi$  interaction. This interaction enhances the stability of the FLCMs monomers, thereby increasing the material's potential for various applications. The provision of triple protection is made possible in FLCMs through the integration of three distinct state-of-the-art photonic components.<sup>96</sup>

## 6. Conclusions and outlook

Cholesteric LC emulsions represent a groundbreaking advancement in the fight against counterfeiting. Their unique ability to respond to external stimuli and form intricate patterns makes them indispensable for creating secure labels and packaging, bolstering product authentication, and reducing fraud risks. These emulsions herald a new era in security technology, fostering innovation in anti-counterfeiting measures with their dynamic, adaptable nature. Imagining a future where safety features evolve akin to chameleons, cholesteric LC emulsions could significantly hinder duplication efforts. Moreover, integrating them with cutting-edge technologies such as blockchain, artificial intelligence, and nanotechnology could establish a robust security network surpassing conventional methods. AI algorithms could swiftly authenticate these emulsions using distinctive fingerprints derived from their structural or topological characteristics. Positioned at the forefront of authenticity protection, cholesteric LC emulsions blend innovation, responsiveness, and aesthetic appeal, revolutionizing the battle against counterfeiting into a dynamic endeavor. However, despite their benefits, cholesteric LC emulsions face challenges. Stability concerns, including potential phase separation or coalescence over time, necessitate stable formulations to ensure consistent performance. The intricate manufacturing process demands precise control over variables like temperature, shear rate, and mixing conditions to achieve uniform droplet size and distribution. Additionally, scaling production while maintaining uniformity poses ongoing difficulties, especially in high-throughput settings. Researchers are actively tackling these obstacles through novel formulation techniques, inventive stabilizing agents, and advancements in LC materials.

In conclusion, the significance of cholesteric LC emulsions as templates for intricate colloidal assemblies is paramount, particularly in the realm of anti-counterfeiting strategies. This overview underscores their vast potential applications and stresses the imperative for continued research to fully unlock their practical capabilities. As these emulsions evolve in sophistication and security, future advancements promise broader deployment across diverse applications, notably in anti-counterfeiting, reaffirming their pivotal role in safeguarding authenticity.

## Abbreviations

CNC	Cellulose nanocrystals
LC	Liquid crystal
SDS	Sodium dodecyl sulfate
CTAB	Hexadecyl trimethyl ammonium bromide
HTP	Helical twisting power
PVA	Polyvinyl alcohol
FCLC	Fluorescent chiral nematic liquid crystal
L-CP	Left-circularly polarized
MF	Melamine-formaldehyde
R-CP	Right-circularly polarized
RECs	Rare-earth complexes
RMes	Reactive mesogens
O/W (W/O)	Oil-in-water (water-in-oil)
O/W/O	Oil-in-water-in-oil
O/W/O/W	Oil-in-water-in-oil-in-water
W/LC/W	Water-in-LC-in-water
LC/F/W (F/LC/W)	LC-in-fluorocarbon-in-water (fluorocarbon-in-LC-in-water)
PC	Photonic crystal
PUF	Physical unclonable functions
PVP	Polyvinylpyrrolidone
CPL	Circularly polarized luminescence
LCPCs	Liquid crystal photonic capsules
RH (LH)	Right handedness (Left handedness)

## Data availability

As this manuscript is a review article, it synthesizes and analyzes data from previously published studies. All the data referenced in this review are available in the original publications, which are cited appropriately throughout the manuscript. The specific data, including figures, tables, and datasets, can be accessed through the respective publications, which are listed in the references section. We encourage readers to refer to these primary sources for further details.

## Conflicts of interest

There are no conflicts to declare.

## Acknowledgements

The authors thank the Director, NIT Warangal for providing research facilities to carry out research work.

## References

- O. Z. Pyzik and I. Abubakar, *Nat. Rev. Dis. Primers*, 2022, **8**, 55.
- J. Helen Ratna Monica, J. Sharma and P. Y. Dave, *J. Adv. Chem. Sci.*, 2021, **7**, 706–710.
- A. Abdollahi, H. Roghani-Mamaqani, M. Salami-Kalajahi, B. Razavi and K. Sahandi-Zangabad, *Carbohydr. Polym.*, 2020, **245**, 116507.



- 4 Q. Kuang, X. Hou, C. Du, X. Wang and D. Gao, *Phys. Chem. Chem. Phys.*, 2023, **25**, 17759–17768.
- 5 Y. Sun, X. Le, S. Zhou and T. Chen, *Adv. Mater.*, 2022, **34**, 2201262.
- 6 K. Muthamma and D. Sunil, *ACS Omega*, 2022, **7**, 42681–42699.
- 7 Y. Liu, L. Zhou, Y. Li, R. Deng and H. Zhang, *Nanoscale*, 2017, **9**, 491–496.
- 8 Y. Liu, F. Han, F. Li, Y. Zhao, M. Chen, Z. Xu, X. Zheng, H. Hu, J. Yao, T. Guo, W. Lin, Y. Zheng, B. You, P. Liu, Y. Li and L. Qian, *Nat. Commun.*, 2019, **10**, 2409.
- 9 M. You, M. Lin, S. Wang, X. Wang, G. Zhang, Y. Hong, Y. Dong, G. Jin and F. Xu, *Nanoscale*, 2016, **8**, 10096–10104.
- 10 K. Jiang, S. Sun, L. Zhang, Y. Lu, A. Wu, C. Cai and H. Lin, *Angew. Chem., Int. Ed.*, 2015, **54**, 5360–5363.
- 11 X. Miao, D. Qu, D. Yang, B. Nie, Y. Zhao, H. Fan and Z. Sun, *Adv. Mater.*, 2018, **30**, 1704740.
- 12 C. Peng, X. Chen, M. Chen, S. Lu, Y. Wang, S. Wu, X. Liu and W. Huang, *Research*, 2021, **2021**, 6098925.
- 13 N. Jaroch, J. Czajka and A. Szczeszak, *Sci. Rep.*, 2023, **13**, 10773.
- 14 D. J. Butler, A. P. Keim, S. Ray and E. Azim, *Nat. Commun.*, 2023, **14**, 5866.
- 15 H. Suo, Q. Zhu, X. Zhang, B. Chen, J. Chen and F. Wang, *Mater. Today Phys.*, 2021, **21**, 100520.
- 16 D. Wang, Z. Liu, H. Wang, M. Li, L. J. Guo and C. Zhang, *Nanophotonics*, 2023, **12**, 1019–1081.
- 17 J. Sun, B. Bhushan and J. Tong, *RSC Adv.*, 2013, **3**, 14862–14889.
- 18 Z. Xuan, J. Li, Q. Liu, F. Yi, S. Wang and W. Lu, *Innovation*, 2021, **2**, 100081.
- 19 M. Stevens and G. D. Ruxton, *Biol. Rev.*, 2019, **94**, 116–134.
- 20 L. Shang, Z. Gu and Y. Zhao, *Mater. Today*, 2016, **19**, 420–421.
- 21 S. Kinoshita and S. Yoshioka, *ChemPhysChem*, 2005, **6**, 1442–1459.
- 22 W. Hong, Z. Yuan and X. Chen, *Small*, 2020, **16**, 1–25.
- 23 S. Tadepalli, J. M. Slocik, M. K. Gupta, R. R. Naik and S. Singamaneni, *Chem. Rev.*, 2017, **117**, 12705–12763.
- 24 L. Shang, W. Zhang, K. Xu and Y. Zhao, *Mater. Horiz.*, 2019, **6**, 945–958.
- 25 H. S. Kang, S. W. Han, C. Park, S. W. Lee, H. Eoh, J. Baek, D.-G. Shin, T. H. Park, J. Huh, H. Lee, D.-E. Kim, D. Y. Ryu, E. L. Thomas, W.-G. Koh and C. Park, *Sci. Adv.*, 2020, **6**, 5769.
- 26 Y. Gong, P. Li, Z. Peng, S. Chen, C. Liu, T. Cheng, J. Fan, J. Niu and W. Lai, *Adv. Opt. Mater.*, 2024, **12**, 2302234.
- 27 M. Mitov, *Soft Matter*, 2017, **13**, 4176–4209.
- 28 A. Abbasi Moud, *ACS Omega*, 2022, **7**, 30673–30699.
- 29 R. Kádár, S. Spirk and T. Nypelö, *ACS Nano*, 2021, **15**, 7931–7945.
- 30 W. Shen, H. Zhang, Z. Miao and Z. Ye, *Adv. Funct. Mater.*, 2023, **33**, 2210664.
- 31 Y. Fu, C. A. Tippetts, E. U. Donev and R. Lopez, *Wiley Interdiscip. Rev.: Nanomed. Nanobiotechnol.*, 2016, **8**, 758–775.
- 32 A. Kumar, U. Dixit, K. Singh, S. Prakash Gupta and M. S. Jamal Beg, *Dyes and Pigments – Novel Applications and Waste Treatment*, IntechOpen, 2021.
- 33 L. Wang, A. M. Urbas and Q. Li, *Adv. Mater.*, 2020, **32**, 1801335.
- 34 M. Mitov, *Advances in Cholesteric Liquid Crystals*, MDPI, 2020.
- 35 M. Urbanski, C. G. Reyes, J. Noh, A. Sharma, Y. Geng, V. Subba Rao Jampani and J. P. F. Lagerwall, *J. Phys.: Condens. Matter*, 2017, **29**, 133003.
- 36 H. K. Bisoyi and Q. Li, *Chem. Rev.*, 2022, **122**, 4887–4926.
- 37 M. Schwartz, G. Lenzini, Y. Geng, P. B. Rønne, P. Y. A. Ryan and J. P. F. Lagerwall, *Adv. Mater.*, 2018, **30**, 1707382.
- 38 P. Kumar, S. Singh and B. K. Gupta, *Nanoscale*, 2016, **8**, 14297–14340.
- 39 A. Abdollahi, H. Roghani-Mamaqani, B. Razavi and M. Salami-Kalajahi, *ACS Nano*, 2020, **14**, 14417–14492.
- 40 P. J. Collings and M. Hird, *Introduction to liquid crystals: Chemistry and physics*, 2017.
- 41 M. Mitov, *Adv. Mater.*, 2012, **24**, 6260–6276.
- 42 P. Zhang, A. J. J. Kragt, A. P. H. J. Schenning, L. T. De Haan and G. Zhou, *J. Mater. Chem. C*, 2018, **6**, 7184–7187.
- 43 B. A. San Jose, J. Yan and K. Akagi, *Angew. Chem., Int. Ed.*, 2014, **53**, 10641–10644.
- 44 X. Yang, X. Jin, T. Zhao and P. Duan, *Mater. Chem. Front.*, 2021, **5**, 4821–4832.
- 45 Q. Xia, L. Meng, T. He, G. Huang, B. S. Li and B. Z. Tang, *ACS Nano*, 2021, **15**, 4956–4966.
- 46 K. Liu, Y. Shen, X. Li, Y. Zhang, Y. Quan and Y. Cheng, *Chem. Commun.*, 2020, **56**, 12829–12832.
- 47 T. J. White, M. E. McConney and T. J. Bunning, *J. Mater. Chem.*, 2010, **20**, 9832–9847.
- 48 H. K. Bisoyi, T. J. Bunning and Q. Li, *Adv. Mater.*, 2018, **30**, 1–35.
- 49 H. Q. Chen, X. Y. Wang, H. K. Bisoyi, L. J. Chen and Q. Li, *Langmuir*, 2021, **37**, 3789–3807.
- 50 F. Goodarzi and S. Zendejboudi, *Can. J. Chem. Eng.*, 2019, **97**, 281–309.
- 51 N. Garti, *Colloids Surf., A*, 1997, **123–124**, 233–246.
- 52 S. S. Lee, H. J. Seo, Y. H. Kim and S. H. Kim, *Adv. Mater.*, 2017, **29**, 1–8.
- 53 M. Pavlovic, M. Antonietti, B. V. K. J. Schmidt and L. Zeininger, *J. Colloid Interface Sci.*, 2020, **575**, 88–95.
- 54 W. Wang, R. Xie, X. J. Ju, T. Luo, L. Liu, D. A. Weitz and L. Y. Chu, *Lab Chip*, 2011, **11**, 1587–1592.
- 55 X. Wang, E. Bukusoglu and N. L. Abbott, *Chem. Mater.*, 2017, **29**, 53–61.
- 56 T. F. Tadros, *Emulsions*, De Gruyter, 2016.
- 57 S. Battat, D. A. Weitz and G. M. Whitesides, *Lab Chip*, 2022, **22**, 530–536.
- 58 L. Y. Chu, A. S. Utada, R. K. Shah, J. W. Kim and D. A. Weitz, *Angew. Chem., Int. Ed.*, 2007, **46**, 8970–8974.
- 59 A. S. Utada, L. Y. Chu, A. Fernandez-Nieves, D. R. Link, C. Holtze and D. A. Weitz, *MRS Bull.*, 2007, **32**, 702–708.
- 60 W. Li, L. Zhang, X. Ge, B. Xu, W. Zhang, L. Qu, C.-H. Choi, J. Xu, A. Zhang, H. Lee and D. A. Weitz, *Chem. Soc. Rev.*, 2018, **47**, 5646–5683.



- 61 Y. Xia and G. M. Whitesides, *Angew. Chem., Int. Ed.*, 1998, **37**, 550–575.
- 62 J. C. McDonald, D. C. Duffy, J. R. Anderson, D. T. Chiu, H. Wu, O. J. A. Schueller and G. M. Whitesides, *Electrophoresis*, 2000, **21**, 27–40.
- 63 R. K. Shah, H. C. Shum, A. C. Rowat, D. Lee, J. J. Agresti, A. S. Utada, L.-Y. Chu, J.-W. Kim, A. Fernandez-Nieves, C. J. Martinez and D. A. Weitz, *Mater. Today*, 2008, **11**, 18–27.
- 64 B. F. B. Silva, C. Rodríguez-Abreu and N. Vilanova, *Curr. Opin. Colloid Interface Sci.*, 2016, **25**, 98–108.
- 65 Y. Geng, J. Noh and J. P. F. Lagerwall, *Proc. SPIE*, 2016, **9769**, 97690U.
- 66 Y. Geng, J. H. Jang, K. G. Noh, J. H. Noh, J. P. F. Lagerwall and S. Y. Park, *Adv. Opt. Mater.*, 2018, **6**, 1700923.
- 67 J. H. Kang, S. H. Kim, A. Fernandez-Nieves and E. Reichmanis, *J. Am. Chem. Soc.*, 2017, **139**, 5708–5711.
- 68 X. Liu, M. G. Debije, J. P. A. Heuts and A. P. H. J. Schenning, *Chem. – Eur. J.*, 2021, **27**, 14168–14178.
- 69 X. Liu, Y. Xu, J. P. A. Heuts, M. G. Debije and A. P. H. J. Schenning, *Macromolecules*, 2019, **52**, 8339–8345.
- 70 J. M. Brake, A. D. Mezera and N. L. Abbott, *Langmuir*, 2003, **19**, 6436–6442.
- 71 I. H. Lin, D. S. Miller, P. J. Bertics, C. J. Murphy, J. J. De Pablo and N. L. Abbott, *Science*, 2011, **332**, 1297–1300.
- 72 S. J. Aßhoff, S. Sukas, T. Yamaguchi, C. A. Hommersom, S. Le Gac and N. Katsonis, *Sci. Rep.*, 2015, **5**, 1–10.
- 73 J. Noh, H. L. Liang, I. Drevensek-Olenik and J. P. F. Lagerwall, *J. Mater. Chem. C*, 2014, **2**, 806–810.
- 74 H. G. Lee, S. Munir and S. Y. Park, *ACS Appl. Mater. Interfaces*, 2016, **8**, 26407–26417.
- 75 A. Concellón, D. Fong and T. M. Swager, *J. Am. Chem. Soc.*, 2021, **143**, 9177–9182.
- 76 B. Gollapelli, A. K. Tatipamula, S. Dewanjee, R. S. Pathinti and J. Vallamkondu, *J. Mater. Chem. C*, 2021, **9**, 13991–14002.
- 77 A. Concellón, C. A. Zentner and T. M. Swager, *J. Am. Chem. Soc.*, 2019, **141**, 18246–18255.
- 78 S. S. Lee, S. K. Kim, J. C. Won, Y. H. Kim and S.-H. Kim, *Angew. Chem., Int. Ed.*, 2015, **127**, 15481–15485.
- 79 P. Sleczkowski, Y. Zhou, S. Iamsaard, J. J. de Pablo, N. Katsonis and E. Lacaze, *Proc. Natl. Acad. Sci. U. S. A.*, 2018, 201720742.
- 80 W. J. Lee, B. Kim, S. W. Han, M. Seo, S. E. Choi, H. Yang, S. H. Kim, S. Jeong and J. W. Kim, *J. Ind. Eng. Chem.*, 2018, **68**, 393–398.
- 81 P. Lin, Q. Yan, Z. Wei, Y. Chen, S. Chen, H. Wang, Z. Huang, X. Wang and Z. Cheng, *ACS Appl. Mater. Interfaces*, 2018, **10**, 18289–18299.
- 82 J. Guo, J. Zhang, Q. Zhang, N. Jiang and J. Wei, *RSC Adv.*, 2013, **3**, 21620–21627.
- 83 J. He, S. Liu, G. Gao, M. Sakai, M. Hara, Y. Nakamura, H. Kishida, T. Seki and Y. Takeoka, *Adv. Opt. Mater.*, 2023, **11**, 202300296.
- 84 H. J. Seo, S. S. Lee, J. Noh, J. W. Ka, J. C. Won, C. Park, S. H. Kim and Y. H. Kim, *J. Mater. Chem. C*, 2017, **5**, 7567–7573.
- 85 T. Yang, D. Yuan, W. Liu, Z. Zhang, K. Wang, Y. You, H. Ye, L. T. de Haan, Z. Zhang and G. Zhou, *ACS Appl. Mater. Interfaces*, 2022, **14**, 4588–4597.
- 86 Y. Geng, J. Noh, I. Drevensek-Olenik, R. Rupp, G. Lenzini and J. P. F. Lagerwall, *Sci. Rep.*, 2016, **6**, 2–10.
- 87 M. Liu, J. Fu, S. Yang, Y. Wang, L. Jin, S. H. Nah, Y. Gao, Y. Ning, C. B. Murray and S. Yang, *Adv. Mater.*, 2022, **35**, 2207985.
- 88 X. Wang, B. Zhao and J. Deng, *Adv. Mater.*, 2023, **35**, 202304405.
- 89 X. Zhan, Z. Zhou, W. Zhou, Y. Yan, J. Yao and Y. S. Zhao, *Adv. Opt. Mater.*, 2023, **11**, 2200872.
- 90 S. Kang, Y. Li, D. Bukharina, M. Kim, H. Lee, M. L. Buxton, M. J. Han, D. Nepal, T. J. Bunning and V. V. Tsukruk, *Adv. Mater.*, 2021, **33**, 2103329.
- 91 S. Lin, Y. Tang, W. Kang, H. K. Bisoyi, J. Guo and Q. Li, *Nat. Commun.*, 2023, **14**, 3005.
- 92 L. Qin, X. Liu, K. He, G. Yu, H. Yuan, M. Xu, F. Li and Y. Yu, *Nat. Commun.*, 2021, **12**, 1–9.
- 93 B. Gollapelli, S. Rama Raju Ganji, A. Kumar Tatipamula and J. Vallamkondu, *J. Mol. Liq.*, 2022, **363**, 119952.
- 94 B. Gollapelli, R. Suguru Pathinti and J. Vallamkondu, *ACS Appl. Nano Mater.*, 2022, **5**, 11912–11922.
- 95 C. Qu, X. Li, N. Zhao, S. Zhou, J. Wang, L.-S. Yao and Y. Liu, *J. Mater. Chem. C*, 2023, **11**, 9649–9656.
- 96 P. Lin, H. Chen, A. Li, H. Zhuang, Z. Chen, Y. Xie, H. Zhou, S. Mo, Y. Chen, X. Lu and Z. Cheng, *ACS Appl. Mater. Interfaces*, 2020, **12**, 46788–46796.

